Exploring Structure and Energetics of a Helix-Forming Oligomer by Molecular Modeling and Molecular Dynamics Simulation Methods: Dynamics of Water in a Hydrophobic Nanotube

ARTICLE *in* THE JOURNAL OF PHYSICAL CHEMISTRY B · OCTOBER 2002

Impact Factor: 3.3 · DOI: 10.1021/jp014730k

1 AUTHOR:

Srikanta Sen

29 PUBLICATIONS **332** CITATIONS

SEE PROFILE

Exploring Structure and Energetics of a Helix-Forming Oligomer by Molecular Modeling and Molecular Dynamics Simulation Methods: Dynamics of Water in a Hydrophobic Nanotube

Srikanta Sen*

Theoretical Biology Group, Human Genetics and Genomics Division, Indian Institute of Chemical Biology, 4 S. C. Mullick Road, Jadavpur, Calcutta-700032, India

Received: December 31, 2001; In Final Form: August 16, 2002

Molecular dynamics simulation studies on the structure, energetics, and dynamics of an *all-meta*-phenylacetylene oligomer in helical and coiled conformations in water have been performed in order to understand the physical basis of helix stabilization in water. It has been demonstrated that the oligomer maintained a dynamically stable helical structure in aqueous solvent at room temperature, without intrachain H-bonds, in agreement with experimental observation. The structure obtained from simulation is found significantly different from the structure presented before based on energy minimization only. The average structure of the helix from dynamics simulation has been characterized in detail. Comparison of energetics between the helical and coiled conformations of the oligomer demonstrated that, in addition to the solvophobic effect, the self-energy of the oligomer also provides a substantial preference toward the helix structure due to favorable van der Waal interactions. No water bridge stabilizing the helix was found. Interestingly, the helix represents a novel model double-walled nanotube (DWNT). Although the inside surface of the helix pore is dominantly hydrophobic in nature, water molecules are allowed to enter into the tube during dynamics but no permeation of water through the tube was observed over the 0.75 ns trajectory. The water molecules inside the hydrophobic tube were found to be strongly H-bonded among them with long lifetimes. The overall dynamics of water inside the tube was quite different from that of water molecules in the bulk.

Introduction

The ordered three-dimensional (3D) structure of a protein is believed to be determined and maintained by a number of competing interatomic interactions. There is a continued debate on the issue of understanding which one of (i) the intrachain H-bonding in the backbone and (ii) the hydrophobic interactions of the side chains of a protein segment plays the major role in driving and stabilizing a α-helix in aqueous solvent. It has been pointed out that the backbone polar groups of a protein segment which are engaged in intrachain H-bonds in α-helical conformation can also participate in H-bonding with the surrounding water molecules when it is in a coiled state in aqueous solvent, and the energetics of the intrachain H-bonding are not generally favorable compared to those of the H-bonding with water.[1,2] On the basis of this argument, it has been proposed that a transition from a random coil conformation to a α-helix will not gain energetically much from H-bonds and hence H-bonding cannot be the major source in driving and stabilizing the α-helix conformation. At present it is believed that the hydrophobic effect of the side chains acts as the main helix-driving force.[1,2] In view of improving our insight in this matter, Nelson et al.,[3] has recently developed a series of novel synthetic oligomers (*all-meta*-phenylacetylene) made of hydrocarbons that differ only in the side chains. The simplest one has a hydrogen atom as the side chain. These oligomers are unique in the sense that its backbones do not contain any H-bond donor and are thus incapable of forming intrachain H-bonds.[3] The chemical structure of the building blocks is given in Figure 1 (inset) indicating a dominantly hydrophobic character of the chain. Nelson et al.,[3] have explicitly shown by experiments using different solvents (acetone, water, along with their mixtures, etc.) that each of these oligomers with different side chains forms a stable helix in aqueous solvent and undergoes a solvent or temperature induced helix-coil transition like a helical peptide. From their observations they have concluded that solvophobic effect alone is quite capable of driving and stabilizing the helical conformation of an oligomer, at least in these particular cases. However, the structural and dynamical characterization of the helix was not done and a detailed analysis of the intramolecular interactions and the solvent effects in aqueous solvent were not presented in full extent at the atomic level. These are the most important issues that must be clarified in improving our insights

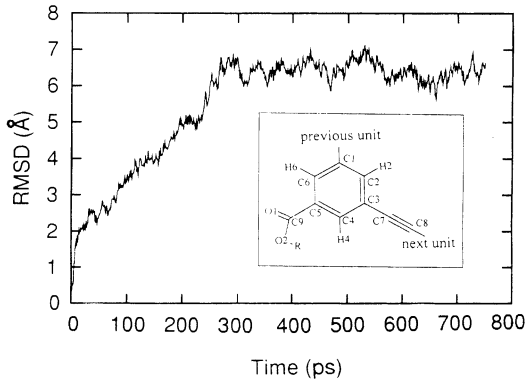

Figure 1. Time evolution of the RMSD of the oligomer in helix conformation during dynamics simulation with reference to its initial energy minimized model conformation. Inset represents the monomeric unit of the oligomer. C1 is connected to C8 of the previous unit, and C3 is connected to the C1 of the next unit to form an oligomer. In the present case, R is a hydrogen atom H21.

* To whom correspondence should be addressed. E-mail: srikanta@chembiotek.com. Present address: Chembiotek Research International, BN Block, Plot 7, Sector-V, Salt Lake City, Calcutta-700091, India.

10.1021/jp014730k CCC: $22.00
Published on Web 10/03/2002

further about the physical basis of their observations and helix stabilization in general.

To make our understanding more complete, in the present paper the issues mentioned above have been addressed in full details by using molecular modeling and molecular dynamics simulation methods on the simplest one of these oligomers where the side chain is a H-atom. The simplest variant of the oligomer has been chosen not only for its simplicity but also due to the fact that in this case the H-atom as the side chain is actually a part of a hydroxyl group and thus capable of forming intrachain H-bonds. Thus, it is important to investigate if this polar H-atom contributes in the helix stability in this case. Molecular modeling (MD) and molecular dynamics (MM) simulation techniques have emerged as powerful tools in investigating the properties of complex molecular systems in full atomic details.[4−15] These methods are particularly useful in investigating molecular properties that are rather difficult to probe experimentally, and thus can be complementary to experimental methods. In the present investigation it would be very straightforward and informative to simulate the complete process of folding. However, it is quite well-known that with the presents day's computational power, it is not very practical to perform MD simulation longer than a few nanoseconds time scale which is far short compared to the usual folding time scale (>microseconds). So, the alternative is to perform MD simulations of the oligomer separately in helix and coiled conformations and compare the energetics and dynamics. In the present work I have performed MD simulations of an oligomer containing 25 residues in helix and coil conformations separately in aqueous solvent at 300 K. We have considered the case of aqueous solvent because it is experimentally found that aqueous solvent stabilizes the helical conformation. The dynamics trajectories were analyzed mainly to (i) characterize the structure and dynamics of the energetically relaxed conformation of the oligomer in helix state and (ii) investigate the interplay of different interactions to understand the physical basis of helix stabilization in this case. Another interesting aspect found in this study is that the surface of the helix pore generated by several hydrophobic atoms of the oligomer represents a hydrophobic nanotube. Such a helix is also novel in the sense that it gives us an additional opportunity to investigate the dynamics and other properties of water molecules inside a hydrophobic nanotube including permeation of water through it. Some interesting results on this aspect have also been presented here.

Methods

Topology and Parameters. To perform MD simulation of the oligomer by the dynamics simulation program package CHARMM-26,[16,17] it is essential to prepare a proper topology for the repeating unit of the new oligomer. For this purpose I have first compared the covalent structure of parts of this new unit (inset Figure 1) with parts of molecules which are largely similar to this unit and are already present in the CHARMM topology file. For example, we have found partial similarity between this unit and the molecular unit ASPP (protonated aspartic acid) and between the residue PHE (phenylalanine) and the six-member ring of the present molecular unit. On the bases of such similarities, the atom types to the different atoms of the new unit were assigned. This makes many of the bond, angle, dihedral, improper, and van der waal parameters directly available from the existing CHARMM-26 parameter file. Other parameters were obtained by comparing with similar cases in CHARMM. The length of the triple bond used is 1.204 Å.[18] The partial atomic charges of the unit were obtained by fitting the charges to the electrostatic potentials at more than 1000 space points by ESP method in MOPAC package version 6.0.[19] The charges are slightly adjusted to make them more consistent with the charges of the atoms in similar parts of other molecular units in CHARMM. A complete list of all the atom types, partial atomic charges, and the additional parameters used here for the unit are presented in Tables 3 and 4 of the appendix.

Generation of the Initial Helix and Coil Conformations and Its Solvation. The coordinates of the atoms of a single unit of this new oligomer were generated by CHARMM with the ring in the $X-Y$-plane.[20] This unit was considered as the first unit of the oligomer in helix conformation. To generate the coordinates of the atoms of the next unit of the oligomer in helix, the coordinates of the previous unit were first rotated about the Z-axis by appropriate angle and then translated in the X−Y-plane such that the relevant atoms (see legend of Figure 1) of this unit and the previous one are positioned in a proper bond distance for covalent continuity. Finally a small shift (0.5 Å) along the Z-direction was given to form a helix avoiding van der Waal clashes between physically nearest units after completion of a full turn. Repeating this process an approximate helix of 25 monomeric units was obtained. There were five units per turn of this modeled helix as was in the original model of Nelson et al.[3] The total potential energy of the helix was minimized in a vacuum by 1000 steepest descent steps in order to minimize the distortions in the generated structure that developed in the construction procedure. This energy-minimized structure was then solvated by placing it at the center of a preequilibrated water sphere of 19.0 Å radius containing 963 TIP3P water molecules.[21] Water molecules whose oxygen atoms were closer than 2.8 Å from any atom of the solute were deleted. After deletion, there were a total of 731 water molecules in the system. This solvated system was further energy minimized by 500 steepest descent steps to remove any bad van der Waal contact between the helix and the water molecules around the helix. The resulting system was then used for subsequent MD simulation following the protocol described in the next section.

As a detailed investigation of the full folding process of a polymer is not yet possible by MD simulation, we need to perform a separate MD simulation for the coiled polymer in order to obtain the energetics of an arbitrarily chosen coiled conformation as a representative of the coiled conformations. The conformation of the oligomer in the coiled state was generated by performing MD simulation of the helix at high temperature ($T = 1000$ K) in a vacuum over a time period of 100 ps. A suitable frame (with RMSD =15.1 Å with respect to the initial helix) was selected from the later part of the trajectory by visualizing it and was energy minimized by 500 steepest descent steps in a vacuum to remove distortions. It was then solvated by adding a 7.0 Å water layer as solvent, to keep the size of the system reasonable. We have shown earlier that such a solvent shell can provide a realistic solvent environment at least for MD simulation over a time period of about 1 ns.[13] The purpose of solvating the coil is to generate coil conformations consistent with an aqueous environment such that the computed solvent accessible surface area in this case can be directly compared to that in the helix sate. The solvated coil was then used for MD simulation.

Simulation Protocol. In the MD simulation of the helix solvated in a water sphere, the water molecules were subjected to a mean-field force resulting from bulk water molecules beyond the 19.0 Å water sphere.[22] This minimizes the finite boundary effect and prevents the surface water molecules from evaporation. In the simulations, Newton's equation of motion for each atom was integrated using the leapfrog algorithm[23,24]

with a time step of 2.0 fs. The SHAKE algorithm[25,26] was applied to constrain the bond lengths involving hydrogen atoms to their equilibrium positions with a tolerance of 0.0001. Spherical cutoff methods were applied in calculating the nonbonded interactions[27] that were smoothly shifted to zero at 12.0 Å. The nonbonded pair list was generated using a cutoff value of 13.0 Å and was updated every 10 steps. For electrostatic calculations a relative dielectric constant 1.0 was used. It may be mentioned here that although the present trend in handling the electrostatic interaction is to use Ewald/PME methods,[28] in the present case I have used spherical cutoff methods along with the force shift method. This is because Ewald/PME methods are not applicable for a spherical solvent setup. However, it is also established now that careful use of force shift cutoff methods in the range (12−14 Å) can produce stable and reliable trajectories in the nanoseconds time scale.[15]

During the MD simulation of the helix in water sphere, the system was heated to 300 K during the first 4 ps and then equilibrated for 4 ps by assigning velocities to the atoms from a Gaussian distribution at 300 K. The simulation was continued with checking the temperature every 100 steps and the temperature was adjusted by scaling velocities only if the average temperature of the system was outside the window (300 ± 10) K. Thus, the average temperature was maintained around 300 K. The trajectory was saved every 100 steps for analysis. MD simulation with the helix in water sphere was continued for 0.75 ns. Structural and dynamical analyses were then performed over the last 400ps of the trajectory. Identical protocol excepting the mean-field boundary force was used for the dynamic simulation of the coiled oligomer solvated with a solvent layer. The simulation was continued for 100 ps only as the purpose was to generate a coil conformation under aqueous environment. All MD simulations were performed by employing the program package CHARMM, version 26 and its parameter set.[16,17] It may be emphasized that in these simulations we have not used any constraints excepting the standard SHAKE for bonds involving H-atoms.

Results and Discussions

Relaxation of the Helix. The time evolution of the root-mean-squared deviation (RMSD) of the coordinates of the helix at each time frame with respect to the coordinates of its initial energy minimized model-built conformation is a standard way to probe the conformational relaxation of a macromolecular system. RMSD is defined as $\mathrm{RMSD}(t,t_0) = \min_{\{\mathrm{rot,trans}\}}[\Sigma\{r_i(t) - r_i(t_0)\}^2/N]^{1/2}$ where $r_i(t)$ and $r_i(t_0)$ represent the position coordinates of the ith atom of the system at the time step t and the reference conformation at t_0 (=0 for the initial conformation), and it is meant that the coordinates of the atoms in the conformation at the time step t is translated and rotated with respect to the reference conformation at time $t_0 = 0$ to minimize the value of the root-mean-squared difference between the two conformations.[29] In the present case, Figure 1 clearly indicates that during dynamics the irregularities and the conformational distortions present in the initial structure have gradually been removed and finally has reached a stable conformation corresponding to an average RMSD value of 6.4 ± 0.2 Å. The reasonably stable nature of the average RMSD value over the last 400 ps of the trajectory ensures that a stable structure has been reached. Similarly, the gradual lowering of the self-energy of the helix also indicates that a proper conformational relaxation has occurred and the molecule has settled down to an energetically more favorable conformation compared to its initial modeled conformation (data not shown). The average self-energy of the oligomer has a reasonably stable value of 40.9 ± 12.3 kcal/mol over the last 400 ps of the trajectory. Self-energy is defined as the potential energy of the helix where the atomic interactions are confined within the helix itself and includes both the bonded (bond, angle, dihedral, improper) and nonbonded (electrostatic and van der Waal) interactions.

Structural and Dynamical Characterization of Helix. A regular and well-defined helical conformation is found as the energy minimized (by 1000 steepest descent steps) structure of the helix averaged over the last 400 ps of the dynamics trajectory as shown in Figure 2a,b in agreement with experimental observation.[3] The self-energy of the average structure after minimization in a vacuum by 1000 steepest descent steps is $E^{a}_{min} = -302$ kcal/mol (Figure 2a,b) which is energetically much favorable compared to the corresponding value ($E^{i}_{min} = -100$ kcal/mol) of the initial model built structure. The stable conformation of the helix is significantly different from the initial model-built structure and the energy minimized structure published before.[3] In the present case, the O1 and O2 atoms of the helix are more uniformly distributed on the helix surface compared to that in ref 3. The average values for the inner and outer diameters of the helix over the stable part of the trajectory are obtained as 9.8 ± 0.1 and 18.7 ± 0.3 Å respectively while the corresponding values in the initial model was 8.6 and 17.7 Å. The inner pore surface is defined by the positions of the C2 atoms and the outer surface is determined by the positions of the O2 atoms and the van dar Waal radii of the relevant atoms have not been considered in this estimate. The helix thus represents a double-walled nanotube (DWNT). The average helix pitch and the average rise are computed as about 5.5 residues per turn and 0.69 Å per residue, respectively. In the relaxed helical conformation there was sliding between the nearest rings of the neighboring turns and thus deviated from the ideal structure with the nearest rings of the neighboring turns perfectly stacked on the top of each other. This sliding is characterized by the distance between the midpoint of the first ring and the foot of the perpendicular of the midpoint of the second ring projected on the plane of the first ring. An average value of 3.65 ± 0.24 Å of this quantity over the stable part of the trajectory indicates a lowering of the area of overlap between stacked rings in the relaxed helix compared to the perfect stacking condition with complete overlap.

The conformations of the oligomer are determined by the three torsional angles defined as α (C2−C3−+C1−+C2), β (C6−C5−C9−O1), and γ (C5−C9−O2−H21). The torsion angle α determines the relative orientation of the two successive rings of the oligomer while, β and γ describe the orientation of the C9−O1 group and the O2−H21 group with reference to the ring to which these are attached as a part of the side chain, respectively. Analysis of the helix trajectory over the last 400 ps indicated that for the different residues, the average value for α varies in the range (−21.5°−3.7°) with RMS fluctuations in the range (±12.6°−±16.4°) over the individual cases. Similarly, β in individual cases varies over a wider range of 0°−180° with an average of 81.1° ± 47.7° and in the range 0° to −180° with an average −76.2 ° ± 39.2°. On the other hand, the average value of the torsion angle γ varies in the range 178.8°−180.2°) with rms fluctuations in the individual cases in the range (±14.6°−±16.94°). The dihedral angle β actually determines the orientation of the C9−O1 bond with respect to the helix and thus indicates its considerably fluctuating nature. The similar values of the average torsion angles α and γ over the different individual residues in the helix and their similar nature of distribution indicate a very regular nature of the helix (Figure 2a). The small fluctuation in the backbone torsion angles

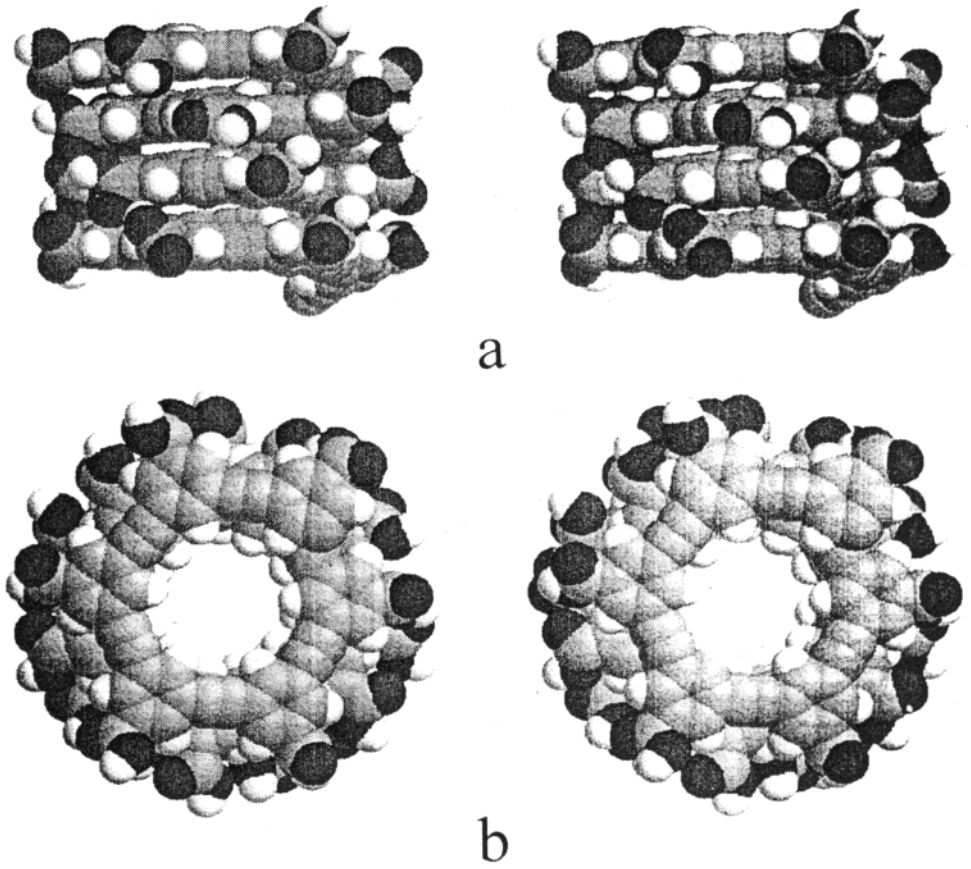

Figure 2. Side (a) and top (b) views for the energy minimized helix, without the end residues, averaged over the last 200 ps of the dynamics trajectory. Gray, black and white color balls represent the carbon, oxygen, and hydrogen atoms, respectively.

and in the RMSD valued during dynamics over the last 400ps of the trajectory indicates that even under a dynamical condition in solution, the helical conformation is well defined leading to a highly packed structure (Figure 2a). The tight structure of the helix as a double-walled nanotube may have important use in nano technology. The reorientational dynamics of the bonds C9−O1 and the O2−H21 bonds which are exposed to the solvent was probed by looking at the correlation function $C(t)$ plots (not shown). $C(t)$ values can be obtained from a dynamics trajectory by the relation $C(t) = \langle P_2(\cos\ \theta(t,\tau))\rangle$ where P_2 represents the second-order Legendre polynomial and $\theta(t,\tau)$ is the angle between the orientations of the bond vector at the initial time and after a period τ. The order parameter S^2 was calculated from the $C(t)$ plot using the relation $C(t) = S^2 + (1 - S^2)\ e^{-t/\tau}$.[30,31] Results show that, in the helix conformation, the reorientational dynamics of the bond vectors C9−O1 and O2−H21 are significantly restricted with S^2 values about 0.4 and 0.8, respectively, while these values for the residues in coiled state are close to zero. This implies that due to close packing in the helix conformation imposes restrictions on the reorientational dynamics of these bond vectors. It is further seen that the dynamics of the bond vector O2−H21 is more restricted compared to that of the bond vector C9−O1. This is possibly caused by the electrostatic interactions between this H21 atom and the oxygen atoms of the nearest neighbor residues on the adjacent turns.

Energetics and Hydration of Helix. It was observed that, during the MD simulation, the energy components due to deformations in bond lengths, dihedral angles, and van dar Waals interactions remain practically unchanged, while the electrostatic energy shows a considerable and systematic improvement due to conformational relaxation (Figure 3a,b).

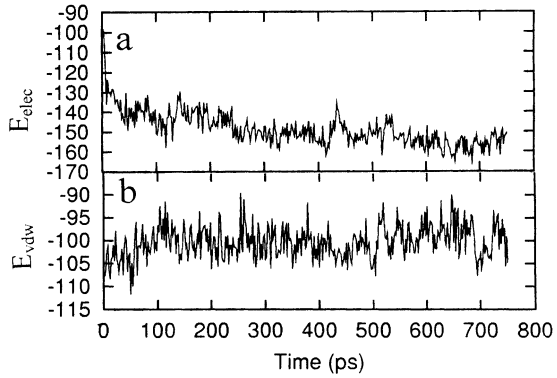

Figure 3. Time evolution of the energy components (electrostatic (a) and van der Waal (b)) of the self-energy of the oligomer in helix conformation. Only the residues in the range 3−23 were considered in these calculations to avoid the end effects.

Thus the relaxation of the electrostatic energy component is the major cause of the structural rearrangements observed in the dynamics simulation. It is also noticeable in Figure 2a that, in the relaxed structure, the highly charged oxygen atoms of each residue is placed at a position between the two oxygen atoms of the neighboring residues of the adjacent turns, and thus reduces the electrostatic repulsion between them compared to the initial model where they were on the top of each other. Moreover, in the present oligomer with a polar H-atom as the side chain, there could be an intrachain H-bond between this H-atom of the hydroxyl group and the O-atoms of the nearest neighbor residue in the adjacent turns. Using the geometric criteria (3.0 Å as distance cutoff and 100° as angle cutoff), we could not find any intrachain H-bonds in such cases. As a typical example, the average distances between the atoms H21 of the

TABLE 1: Comparison of the Solvent Accessible Surface Area (SASA) of the Charged and Hydrophobic Atoms between the Helix and Coil Conformations of the Oligomer

conformation	$SASA_{hydro}$ (Å^2)	$SASA_{charge}$ (Å^2)	$SASA_{total}$ (Å^2)
coil	2883 ± 21	2375 ± 18	5260 ± 24
Helix	1427 ± 45	1771 ± 42	3198 ± 54
ΔSASA	1456	605	2062

residue no 12 and O1 (O2) of the spatially nearest neighboring residues nos. 17 and 18 are obtained as 8.2 Å ± 1.6 Å (8.3 Å ± 1.7 Å) and 6.3 Å ± 1.4 Å (5.8 Å ± 1.5 Å), respectively. The corresponding angles O2−H2···O1 (O2) are about 67.5°± 13.0° (66.2° ± 13.4°) and 79.4° ± 14.3° (81.4° ± 15.7°), respectively, indicating no strong intrachain H-bonds involving these hydrogen atoms.

In the cases of biomolecules, the structures are commonly found to be stabilized by formation of water bridges where at least a single water molecule makes H-bonds simultaneously with two atoms of different parts of the chain molecule. Analyzing the trajectory we did not find any such water bridge of significant lifetime and energies. The time variation of the interaction energy of water and the helix (data not shown) indicates a rapid growth of favorable interaction over the first few tens of picoseconds representing mainly the proper reorientation of the surrounding water molecules to maximize their interactions with the atoms, such as O1, and O2 of the exposed parts of the oligomer. However, the solvent interaction was found to remain fairly constant over the later part of the simulation (data not shown).

Comparison of Energetics between Helix and Coiled States of the Oligomer. The average solvent accessible surface areas (SASA) of the molecule in the helix and coil states, were computed by the method of Richard and Lee using a probe size of 1.6 Å.[32] Calculation over the stable parts of the respective trajectories indicates that there is a considerable degree of reduction in the SASA value due to a transition from coil state (5260 Å^2 ± 24 Å^2) to a helix state (3198 Å^2 ± 54 Å^2) (Table 1). Further analysis shows that the reduction in the SASA for the highly charged atoms (O1, O2) $\Delta SASA_{charge}$ ($= SASA^h_{charge} - SASA^c_{charge}$) is 605 Å^2. On the other hand, the SASA for the hydrophobic (small charge) atoms $\Delta SASA_{hydro}$ ($= SASA^h_{hydro} - SASA^c_{hydro}$) is obtained as 1456 Å^2 which is 2.4 times larger than $\Delta SASA_{charge}$ (see Table 1). Thus, the coil → helix transition is accompanied by a larger reduction in solvent exposure of nonpolar atoms compared to that of the polar or charged atoms. The free energy difference due to solvent effect ($\Delta G_{solv} = G^h_{solv} - G^c_{solv}$) can be estimated using the relation (ΔG_{solv}) = $\Delta SASA_{charge}\sigma_{charge} + \Delta SASA_{hydro}\sigma_{hydro}$, where σ_{charge} and σ_{hydro} represent the surface free energy factors for the charged and hydrophobic atoms, respectively. Using $\sigma_{charge} = -0.06$ and $\sigma_{hydro} = 0.012$,[33] $\Delta G_{solv} = -13.9$ kcal/mol was obtained. This clearly points toward a solvophobic effect favoring the helix-state over the coiled conformation in agreement with the experimental data.[3] On the other hand, comparison of the average self-energies of the polymer in helix ($E^h_{self} = 41 \pm 12$ kcal/mol) and coiled ($E^c_{self} = 87 \pm 10$ kcal/mol) conformational states indicates that from the self-energy point of view the helix conformation is also more favored than the coiled state in this case even in a dynamical environment. To identify which component of the self-energy of the oligomer makes the helix conformation more favorable than the coil conformation, the average values of the major components of the self-energy of the oligomer in helix and coil conformations have been compared as given in Table 2. It is clearly seen that the covalent energy terms are quite similar in both the two conformations. The electrostatic

TABLE 2: Comparison of the Average Values of the Major Components of Self-Energy of the Oligomer in Helix and Coiled Conformations[a]

conformation	bond	angle	dihedral	van der Waal	electrostatic
helix	71 ± 6	96 ± 7	89 ± 5	-101 ± 4	-151 ± 5
coil	75 ± 6	102 ± 8	90 ± 5	-48 ± 3	-166 ± 3

[a] The energies are expressed in kcal/mol.

interaction makes helix slightly unfavorable over coil mostly due to the stronger electrostatic repulsion between the oxygen atoms of the neighboring turns of the helix. On the other hand, the van der Waal interaction strongly favors the helix conformation (Table 2) making the overall preference toward the helix. Thus, in this study it is demonstrated that the helix is stabilized not only by solvophobic effect but also by a significant favorable contribution from the self-energy of the oligomer due to van der Waals interaction which is consistent with the view that several interactions together determines the structural preference.[3] It may be pointed out that for comparing the self-energies between the helix and the coiled states of the oiligomer, we have not considered their interactions with the solvent. This is

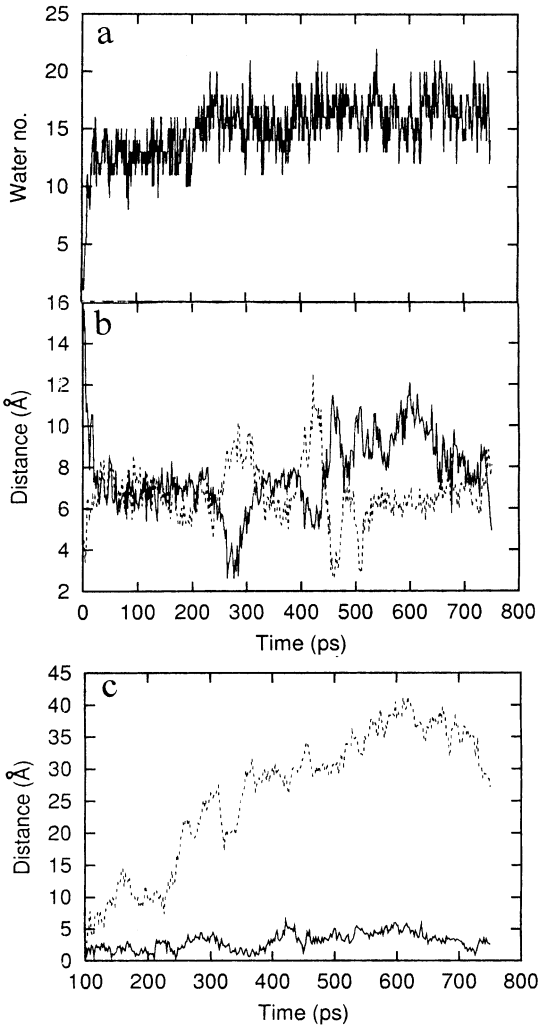

Figure 4. (a) Time evolution of the number of water molecules inside the tube of the helix. (b) Time evolution of the distances of a typical water molecule that entered into the helix tube from the two different ends of the tube as a typical case showing the motion of water inside the tube. The atoms C2 of the residues nos. 5 and 20 are used as the reference points representing the two ends of the nanotube. (c) Comparison of the displacements of a water molecule inside the tube with reference to its position at time 100 ps (solid line) and the same for a water molecule in the bulk (dotted line).

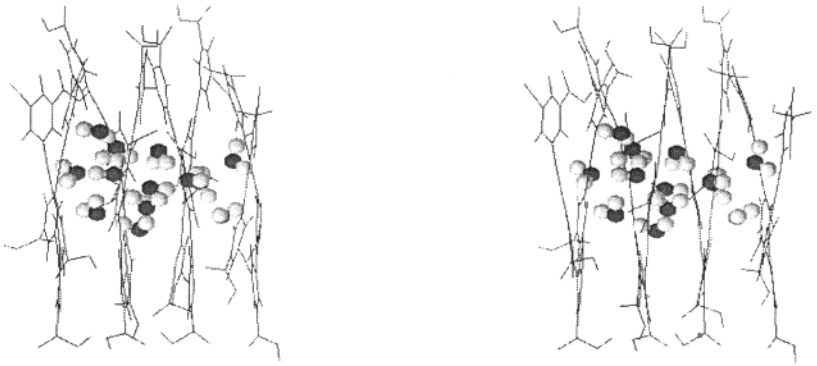

Figure 5. Stereo view of a snapshot from the trajectory to show the relative orientation and positions of the waters inside the nanotube (end residues are not shown).

done to avoid double counting of this contribution, as this effect is already taken care of through the free energy calculation using solvent accessible surface area of the different atoms in the helical and coiled conformations of the oligomer.

Properties of Water in the Hydrophobic Nanotube. It is interesting to point out that the inside part of the helix pore (∼1 nm diameter) is quite hydrophobic in nature due to the presence of the nonpolar atoms such as C2, H2, etc. Thus, this helix pore may be considered as a novel model of hydrophobic nanotube. Initially, in the solvated helix there was no water molecule inside the pore. It was then of natural interest to investigate if under a dynamical environment the hydrophobic tube allows water molecules to enter in it and permeate through it. Figure 4a represents the variation of the number of the water molecules inside the helix tube with time. It is found that during the dynamics simulation water molecules spontaneously started entering the tube and very rapidly reached a stable average number 16.1 ± 2.0. We consider a water molecule to be inside the tube if its oxygen atom is not farther than 3.0 Å from the H2 atom of residues in the range 6−20. The end residues have been excluded to avoid considering the water caps at the two ends that are outside the tube. By detailed analysis we found that in most cases, the water molecules at the face of the tube ends, entered from one end of the tube and exited through the same end after staying there for a time varying in the range of (10−100) ps causing significant fluctuations in the computed number of water molecules inside the tube. This is true for water enering the tube from both ends. However, no case was found where a water molecule permeated through the nanotube entering through one end and exiting through the other within the 0.75 ns time scale of the dynamics simulation. In some of the cases it is found that once entered the water molecule remained inside the tube entirely over the later part of the simulation. Monitoring the time dependence of the distances of such water molecules from both ends indicate that inside the tube such a water molecule moves little and stayed well within the tube (Figure 4b). In contrast to the displacement of a water molecule inside the tube with reference to its reference position at the time frame at 100ps, the corresponding displacement of a water molecule in the bulk water over the last 650ps of the trajectory is very large (∼40 Å) as expected (Figure 4c) indicating large difference in dynamics. The water molecules inside the tube mostly cluster together by forming strong H-bonds among themselves (Figure 5). Time evolution of the radius of gyration R_{gy} of the water molecules inside the tube (selected from a time frame) over the entire period of simulation indicates that the R_{gy} value for the water molecules when inside the tube are small and less fluctuating (Figure 6). This indicates the stable nature of the shape and size of the strongly H-bonded

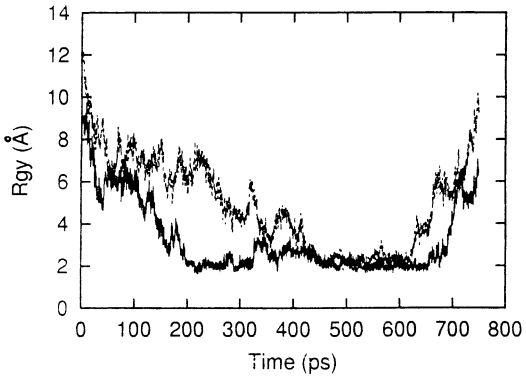

Figure 6. Time evolution of the radius of gyration (R_{gy} of a group of water molecules (found inside the tube at the time frame 560ps) over the entire period of simulation.

water network inside the tube. The time evolution of the R_{gy} for water molecules inside the tube also indicates that after forming a H-bonded structure for a considerable time, some of the water molecules are detached from the water cluster with a large increase in the R_{gy} value (Figure 6). It must be pointed out that in bulk water the lifetime of the H-bond between two nearby water molecules is only a few picoseconds, while inside the nanotube, it is found to be more than 100 ps in many cases. In the present study it is thus clearly demonstrated that the water molecules inside the hydrophobic nanotube have quite different properties compared to that in the bulk water. Apparently, the present results are also indicative of the possibility that such a nonpolar nanotube effectively creates significant resistance in permeating water molecules through it compared to the motion of water molecules in bulk solvent. As a result, water molecules may get trapped inside the tube for a significantly long time. In the present case a few water molecules were found to remain inside the tube starting from a time less than 100 ps until the end of the simulation. It may also be pointed out that although the tube wall restricts the movement of water molecule inside the nanotube, the water molecules are free to move along the axial direction of the tube. Considering the tube pore diameter of about 10 Å, which is significantly large than the diameter (∼3 Å) of water molecule indicates the possibility of considerable movement along the tube axis and hence permeation through the tube. Even if we consider the H2 atoms to define the inside surface of the helix pore, the pore diameter becomes ∼8 Å, which is still 2.7 times larger than the diameter of the water molecules. However, observation of no water permeation through the tube and very little displacement of water inside the tube indicates that not only the tube boundary but also the hydrophobic nature of the inside surface of the nanotube influences the dynamics of water inside the nanotube in this

case. Such a situation is very likely and recently works[34,35] have been reported indicating significantly different behaviors of water molecules in hydrophobic environments of nano range. These interesting features deserve more detailed investigations using longer helix and MD simulation over longer time period.

In a recent work[36] a detailed simulation of the dynamics of water molecules in a carbon nanotube has been reported where the authors have observed significant permeation of water molecules through the carbon nanotube. Permeation of water molecules occurred in bursts in a time scale of a few nanoseconds. However, their observation apparently contrasting to our results may be due to a number of differences between their system and our system; for example, the two systems are quite different from the physicochemical point of view: the nanotube in our case is more heterogeneous as chemical compositions are concerned. The diameters of the inside pores and the tube lengths are different. The water molecules inside the carbon nanotube formed an one-dimensional wire-like H-bonded arrangement, while in our case the helix pore being larger, the water molecules there formed a H-bonded cluster. Finally and most importantly, the time scales of dynamics simulations are largely different; the simulation in the case of carbon nanotube was performed over 66 ns, which is much longer compared to the time period (0.75 ns) in our case. Moreover, the helix being stabilized by nonbonded interactions are more flexible compared to the carbon nanotube.[36] The value of the nonbonded cutoff (13 Å) used in the present simulation also might have some effect on the water permeation through the nanotube of the helix even though the effective length of the nanotube is about 11 Å. Further investigations on these issues should be done in future.

Summary and Conclusions

The main results and conclusions from the present molecular modeling and MD simulation study may be summarized as below.

The oligomer formed a stable helical structure in aqueous solvent at room temperature in agreement with experimental observation. However, its relaxed structure is considerably different from the structure obtained by energy minimization only as presented before. The helical structure of the oligomer is characterized by a helical pitch of about 5.5 residue per helical turn and a rise of 0.69 Å per residue. The helix has a wide inner pore of diameter of about 10 Å and the outer surface of the helix has a diameter of about 19 Å. Each of the relevant torsion angles α, β, and γ has their average values very similar over the different residues implying a regular structure. The small fluctuations of these values about the average values imply a dynamically stable nature of the helical structure that may have important applications in nanotechnology. Only the torsion angle β varies over a wider range. The bond orientational dynamics for the bonds C9−O1 and O2−H21 are considerably restricted in helix conformation while those are free in coiled state.

The electrostatic repulsion between the oxygen atoms of the neighboring turn mainly caused the nearest rings of the adjacent turns to slide away from their perfect stacking configuration. It is demonstrated that the helix is not only stabilized by the solvophobic effect but also by a favorable contribution from the self-energy of the oligomer due to van der Waals interactions in helix conformation. No water bridge or intrachain H-bond (involving side chain H-atom) was found to stabilize the helix further.

Even though the inside of the helix pore represents a dominantly hydrophobic nanotube, water molecules were allowed to enter inside it during dynamics but no permeation of water was observed over the 0.75 ns trajectory. The water molecules inside the tube were found to be strongly H-bonded among them over very large time periods compared to the waters in the bulk. The dynamics of water inside the tube was quite different from that of water molecules in the bulk and requires further studies.

Acknowledgment. This work was supported by the Council of Scientific and Industrial Research, India (under the scientist Pool scheme).

Appendix

TABLE 3

atom name	atom type	partial atomic charge
C1	CA	0.02
C2	CA	−0.15
C3	CA	0.02
C4	CA	−0.15
C5	CA	−0.12
C6	CA	−0.15
C7	CT	0.10
C8	CT	0.10
C9	CD	0.15
O1	OB	−0.30
O2	OH1	−0.33
H2	HP	0.17
H4	HP	0.17
H6	HP	0.17
H21	H	0.30

TABLE 4: Parameters: In CHARMM Parameter Format

Bond

atom 1	atom 2	force constant (kcal/mol/Å^2)	equilibrium value (Å)
CA	CD	250.0	1.490
CA	CT	250.0	1.490
CT	CT	500.0	1.024

Angle

atom 1	atom 2	atom 3	force constant (kcal/mol/rad^2)	equilibrium value (deg)
CA	CA	CT	52.0	120.0
CA	CT	CT	500.0	180.0
CA	CA	CD	52.0	120.0
OB	CD	CA	70.0	125.0
OH	CD	CA	55.0	110.5

Dihedral

atom 1	atom 2	atom 3	atom 4	force constant (kcal/mol)	multiplicity	equilibrium value (deg)
CD	CA	CA	A	3.1	2	180.0
OB	CD	CA	CA	0.4	1	180.0
OH1	CD	CA	CA	0.4	1	180.0
HP	CA	CA	CA	4.2	2	180.0
CA	CA	CD	CA	3.1	2	180.0
CT	CA	CA	CA	3.1	2	180.0
CT	CT	CA	CA	3.1	2	180.0
CA	CT	CT	CA	3.1	2	180.0
HP	CA	CA	CT	4.2	2	180.0

Improper

atom 1	atom 2	atom 3	atom 4	force constant (kcal/mol/rad^2)	multiplicity	equilibrium value (deg)
HP	CA	CA	CA	4.0	0	0.0
CA	CA	CA	CA	4.0	0	0.0
CA	CA	CD	CA	90.0	0	0.0
CT	CA	CA	CA	90.0	0	0.0

References and Notes

(1) Kauzmann, W. *Adv. Protein Chem*. **1969**, *14*, 1−63.
(2) Dill, K. *Biochemistry* **1990**, *29*, 7133−7155.
(3) Nelson, J. C.; Saven, J. G.; Moore, J. S.; Wolynes, P. G. *Science* **1997**, *277*, 1793−1796.
(4) McCammon, J. A.; Harvey, S. C. *Dynamics of Proteins and Nucleic Acids*; Cambridge University Press: London, 1987.
(5) Brooks, C.; Karplus, M.; Pettit, B. M. *Proteins: A Theoretical Perspective on Structure, Dynamics and Thermodynamics*. Wiley: N. W., 1988.
(6) Leach, A. *Molecular Modeling: Principles and Applications*; Addison-Wesly Longman Ltd: Reading, MA, 1996.
(7) Brooks, C. L., III; Karplus, M. *J. Mol. Biol* **1989**, *208*, 159−181.
(8) Feig, M.; Pettitt, B. M. *J. Phys. Chem. B.* **1997**, *101*, 7361−7363.
(9) Andrews B. K.; Romo, T.; Clarage, J. B.; Pettitt, B. M.; Phillips, G. N. *Structure* **1998**, *6*, 587−594.
(10) Sprous, D.; Young, M. A.; Beveridge, R. L. *J. Phys. Chem. B.* **1998**, *102*, 4658−4667.
(11) Sen, S.; Nilsson, L. A. *J. Am. Chem. Soc*. **1998**, *121*, 619−631.
(12) Caflisch, A.; Karplus, M. *Structure* **1999**, *7*, 477−488.
(13) Sen, S.; Nilsson, L. *Biophys. J*. **1999**, *77*, 1782−1800.
(14) Sen, S.; Nilsson, L. *Biophys. J*. **1999**, *77*, 1801−1810.
(15) Cheatham T. E.; Kollman, P. E. *Annu. Rev. Phys. Chem*. **2000**, *51*, 435−471.
(16) Brooks, B. R.; Bruccoleri, R. E.; Olafson, B. D.; States, D. J.; Swaminathan, S.; Karplus. M. *J. Comput. Chem*. **1983**, *4*, 187−217.
(17) MacKerell, A. D., Jr.; Wirkiewicz-Kuczera, J.; Karplus, M. *J. Am. Chem. Soc.* **1995**, *117*, 11946−11975.
(18) Weast, R. C., Ed. *Handbook of Chemistry & Physics (1985−1986)*, 66th ed.; CRC Press: p F-165.
(19) Coolidge, M. B.; Stewart, J. J. P. *MOPAC, version 6.0*; 1990.
(20) Brunger, A.; Karplus, M. *Struct. Funct., Genet*. **1988**, *4*, 148−156.
(21) Jorgensen, W. L.; Chandrasekhar, J.; Madura, J. D.; Impey, R. W.; Klein, M. *J. Chem. Phys*. **1983**, *79*, 926−935.
(22) Brooks, C. L., III; Karplus, M. *J. Chem. Phys*. **1983**, *79*, 6312−6325.
(23) Hockney, R. W. *Methods Phys.* **1970**, *9*, 136−211.
(24) Potter, D. *Computational Physics*; Wiley: New York, 1972; Chapter 5.
(25) Rykaert, J. P.; Ciccotti, G.; Berendsen, H. J. C. *J. Comput. Phys.* **1977** *23*, 327−341.
(26) van Gunsteren, W. F.; Berendsen, H. J. C. *Mol. Phys*. **1977**, *34*, 1311−1327.
(27) Steinbach, P. J.; Brooks, B. R. *J. Comput. Chem*. **1994**, *15*, 667−683.
(28) Daren, T. A.; York, D. M.; Pedersen, L. G. *J. Chem. Phys*. **1993**, *98*, 10089−190092.
(29) Stella, L.; Melchionna, S. *J. Chem. Phys.* **1998**, *109*, 10115−10117.
(30) Lipari, G.; Szabo, A. *J. Am. Chem. Soc.* **1982**, *104*, 4546−4559.
(31) Lipari, G.; Szabo, A. *J. Am. Chem. Soc.* **1982**, *104*, 4559−4570.
(32) Lee, B.; Richard, F. M. *J. Mol. Biol*. **1972**, *55*, 379−400.
(33) Eisenberg, D.; Mclachalan, A. D. *Nature* **1986**, *319*, 199−203.
(34) Koga, K.; Zeng, X. C.; Tanaka, H. *Phys. Rev. Lett*. **1997**, *79*, 5262−5265.
(35) Koga, K.; Tanaka, H.; Zeng, X. C. *Nature* **2000**, *408*, 564−567.
(36) Hummer, G.; Rasaiah, J. C.; Noworyta, J. P. *Nature* **2001**, *414*, 188−190.